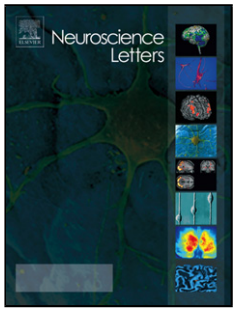

Title: Expression of a dynamin 2 mutant associated with Charcot-Marie-Tooth disease leads to aberrant actin cytoskeleton and lamellipodia formation

Author: Hiroshi Yamada Kinue Kobayashi Yubai Zhang Tetsuya Takeda Kohji Takei

PII: S0304-3940(16)30439-6
DOI: http://dx.doi.org/doi:10.1016/j.neulet.2016.06.030
Reference: NSL 32118

To appear in: *Neuroscience Letters*

Received date: 7-5-2016
Revised date: 3-6-2016
Accepted date: 16-6-2016

Please cite this article as: Hiroshi Yamada, Kinue Kobayashi, Yubai Zhang, Tetsuya Takeda, Kohji Takei, Expression of a dynamin 2 mutant associated with Charcot-Marie-Tooth disease leads to aberrant actin cytoskeleton and lamellipodia formation, Neuroscience Letters http://dx.doi.org/10.1016/j.neulet.2016.06.030

Expression of a dynamin 2 mutant associated with Charcot-Marie-Tooth disease leads to aberrant actin cytoskeleton and lamellipodia formation

Highlights

The expression of dynamin mutants 555Δ3 and K562E decreased lamellipodia formation.

The K562E mutation caused the disappearance of radially aligned actin bundles.

The K562E mutation caused the appearance of F-actin clusters.

Short F-actin assembled into immobile F-actin clusters in K562E-expressing cells.

Hiroshi Yamada, Kinue Kobayashi[a], Yubai Zhang, Tetsuya Takeda, Kohji Takei[*]

Department of Neuroscience, Okayama University Graduate School of Medicine, Dentistry and Pharmaceutical Sciences, 2-5-1 Shikata-cho, Kita-ku, Okayama 700-8558, Japan; and CREST, Japan Science and Technology Agency, 2-5-1 Shikata-cho, Kita-ku, Okayama 700-8558, Japan

[a]Present address: *Department of Molecular Oncology, Institute of Development, Aging and Cancer, Tohoku University, 4-1, Seiryou-machi, Aoba-ku, Sendai, Miyagi 980-8575, Japan*

[*]*All correspondence should be addressed to: Dr. Kohji Takei, Department of Neuroscience, Graduate School of Medicine, Dentistry and Pharmaceutical Sciences, Okayama University, Okayama 700-8558, Japan*

Tel: (+81)-86-235-7120; Fax: (+81)-86-235-7126; e. mail: kohji@md.okayama-u.ac.jp

Running title: Perturbation of the actin cytoskeleton by dynamin 2 CMT mutation

Abstract

Specific mutations in dynamin 2 are linked to Charcot-Marie-Tooth disease (CMT), an inherited peripheral neuropathy. However, the effects of these mutations on dynamin function, particularly in relation to the regulation of the actin cytoskeleton remain unclear. Here, selected CMT-associated dynamin mutants were expressed to examine

their role in the pathogenesis of CMT in U2OS cells. Ectopic expression of the dynamin CMT mutants 555Δ3 and K562E caused an approximately 50% decrease in serum stimulation-dependent lamellipodia formation; however, only K562E caused aberrations in the actin cytoskeleton. Immunofluorescence analysis showed that the K562E mutation resulted in the disappearance of radially aligned actin bundles and the simultaneous appearance of F-actin clusters. Live-cell imaging analyses showed F-actin polymers of decreased length assembled into immobile clusters in K562E-expressing cells. The K562E dynamin mutant colocalized with the F-actin clusters, whereas its colocalization with clathrin-coated pit marker proteins was decreased. Essentially the same results were obtained using another cell line, HeLa and NG108-15 cells. The present study is the first to show the association of dynamin CMT mutations with aberrant actin dynamics and lamellipodia, which may contribute to defective endocytosis and myelination in Schwann cells in CMT.

Keywords: Charcot-Marie-Tooth disease, dynamin, actin, stress fiber, endocytosis.

1. Introduction

Charcot-Marie-Tooth disease (CMT) is a hereditary motor and sensory neuropathy. Two types of CMT show an autosomal dominant inheritance pattern, namely CMT1 and CMT2. CMT1 is characterized by demyelination and nerve conduction deficits, whereas CMT2 results from axonal abnormalities leading to decreased amplitude of neuronal transmission. There are four kinds of intermediate subtypes, namely, dominant intermediate (DI)-CMTA, DI-CMTB, DI-CMTC and DI-CMTD, which show demyelination and aberrant axonal forms [1]. Dynamin 2 is one of the disease-causing genes in DI-CMTB [2].

Dynamin is classified into three isoforms designated as 1–3 [3]. Dynamin 1 is mainly localized in neurons, whereas dynamin 3 is highly expressed in neurons, lung and testis. Dynamin 2 is ubiquitously expressed. Dynamins have common functional domains including a GTPase domain at the N-terminus, a middle domain, a Pleckstrin homology (PH) domain, a GTPase effector domain (GED), and a proline/arginine rich domain (PRD) located at the C-terminus [4]. Dynamins are involved in the process of membrane fission during endocytosis [4].

Dynamins also regulate cytoskeleton dynamics including actin [4] and microtubule [5] dynamics. Dynamin participates in the formation of actin-rich structures, including lamellipodia and dorsal membrane ruffles, invadopodia, podosomes, growth cones, and phagocytic cups [4]. Dynamins directly and indirectly control actin dynamics. Actin bundling mediated by dynamin and cortactin, an F-actin binding protein, stabilizes growth cone filopodia [6]. Crosslinking of F-actin by dynamin and cortactin is involved in intracellular F-actin organization [7]. Furthermore, dynamin alone directly binds to actin filaments and changes the higher order structure of F-actin [8].

Eight CMT-associated mutations in dynamin 2 have been reported to date [9]. These mutations occur mainly at the PH domain, which is the binding motif for phosphoinositide binding. Mutations have also been detected in the middle and PRD domains [9]. Analysis of fibroblasts derived from CMT patients or cells expressing CMT mutant dynamin 2 showed that mutations in the PH domain lead to defective endocytosis of surface receptors, including EGF and transferrin receptors [10,11]. In

particular, the dynamin 2 K562E mutant shows severely inhibited endocytosis [11]. The dynamin 2 CMT mutation 555Δ3 results in alterations in the microtubule cytoskeleton [2] that affect microtubule-dependent membrane transport [5]. The physiological significance of dynamin in the regulation of actin underscores the need to analyze the role of dynamin mutants in CMT and their effect on actin dynamics.

In the present study, the effects of ectopic expression of two selected dynamin 2 CMT mutants, 555Δ3 and K562E, on intracellular actin dynamics were investigated by immunofluorescence and live imaging with Total Internal Reflection Fluorescence microscopy (TIRFM).

2. Materials and Methods

2.1. Antibodies

Polyclonal rabbit anti-V5 antibody (AB3792) and mouse monoclonal antibody against α-adaptin (AP-2) (CP46) were purchased from Life Technologies (Carlsbad, CA). Mouse monoclonal anti-clathrin heavy chain antibody (MA1-065) was from Thermo Fisher Scientific (Waltham, MA). Alexa 488- or Rhodamine Red X-conjugated anti-rabbit IgG or anti-mouse IgG, and Alexa Fluor 488- or Rhodamine-phalloidin were purchased from Life Technologies (Carlsbad, CA).

2.2. cDNA constructs

Rat dynamin 2 wild-type (WT), 555Δ3 or K562E were cloned into pcDNA4 V5/His as previously described by Tanabe et al. [5]. Rat dynamin 2 WT was subcloned into pIRES2-DsRed2 as an EcoRI-SmaI fragment (Clontech Laboratories, Inc., Santa Clara, CA). Mutations were introduced with QuikChange II XL (Agilent Technologies, Santa Clara, CA) in accordance with the manufacturer's instructions, and sequences were verified by DNA sequencing.

2.3. Cell culture and transfection

U2OS (ATCC No; HTB96) cells were cultured in Dulbecco's modified Eagle's medium (DMEM; Life Technologies) supplemented with 10% fetal bovine serum (FBS; Life Technologies) at 37ºC in humidified air with a 5% CO_2 atmosphere. For transfection, U2OS cells were cultured in a six-well plate at a density of 0.5×10^5/well and transfected with 0.25 μg of cDNA of dynamin 2 WT, 555Δ3 or K562E cloned into a pIRES2-DsRed2 expression vector (Clontech Laboratories, Inc.) using Lipofectamine 2000, and then cultured for 32 h. The cells were cultured with 0.2% FBS/DMEM for more than 16 h and stimulated with 10% serum. After 40 min, the cells were fixed and stained as described below. To examine colocalization of dynamin with F-actin cluster, AP-2 or clathrin, U2OS cells were transfected with pcDNA4 V5/His harboring dynamin 2 WT or mutants. Then, serum-stimulated cells were fixed and stained.

2.4. Fluorescent microscopy

Cells were fixed with 4 % paraformaldehyde and stained by immunofluorescence as described previously [6]. Transfected cells were identified by DsRed fluorescence. Samples were examined using a spinning disc confocal microscope system (CSU10, Yokogawa Electric Co., Tokyo, Japan) combined with an inverted microscope (IX-71, Olympus Optical Co., Ltd., Tokyo, Japan) and a CoolSNAP-HQ camera (Roper Industries, Sarasota, FL). The confocal system was controlled by MetaMorph Software (Molecular Devices, Sunnyvale, CA). When necessary, images were processed using Adobe Photoshop CS3 or Illustrator CS3 software.

2.5. Live imaging

U2OS cells were co-transfected with LifeAct-GFP2 (ibidi GmbH, Planegg, Germany) and pIRES2-DsRed2 harboring dynamin 2 WT or K562E. For live imaging, the transfected cells were cultured and stimulated with 10% FBS as described above. The stimulated cells were captured using TIRFM. Dynamin 2 WT or mutant-expressing cells were identified by DsRed fluorescence. Time-lapsed images were acquired with an inverted microscope (IX-71) and a CoolSNAP-Pro camera. Images were automatically captured every 10 seconds and processed by MetaMorph software.

2.6. Morphometry

To investigate lamellipodia formation, cells were stained with Alexa 488 Fluor-phalloidin, and analyzed by fluorescence confocal microscopy. F-Actin-rich protrusive membrane sheets at the leading edge were defined as lamellipodia [12]. Cells with lamellipodia were counted. Ratio value of the number of cells with lamellipodia to total number of counted cells was expressed.

F-actin clusters were identified by visual inspection, and the number of F-actin clusters was counted from images of cells stained with Alexa Fluor 488-phalloidin. Average of the number of F-actin clusters per cell was expressed. Data were analyzed in 33–53 cells from three experiments. All morphometric data were expressed as the mean ±

S.E.M.

2.7. Statistical analysis

Data were analyzed for statistical significance using KaleidaGraph software (version 4.1) for the Macintosh (Synergy Software Inc., Essex Junction, VT, USA). Analysis of variance and Tukey's honest significant difference post hoc test were applied for more than two different groups, and Student's *t*-test was applied for two different groups. *P* values of <0.01 (**) were considered significant.

3. Results

3.1. Expression of the dynamin 2 CMT mutant K562E results in aberrant actin filament structures

To investigate the effect of dynamin 2 mutations associated with CMT on the actin cytoskeleton, two dynamin 2 CMT mutants, namely 555Δ3 and K562E, were expressed in U2OS cells and intracellular F-actin distribution was assessed (Fig. 1A). DsRed2 was co-expressed to identify cells expressing the exogenous proteins. The actin cytoskeleton is remodeled in U2OS cells upon serum stimulation, which facilitates observation of intracellular actin dynamics [7,13].

Upon serum stimulation, U2OS cells formed typical lamellipodia, an extended membrane protrusion. The lamellipodia were supported by higher order actin structures, including radially and transversely arranged actin bundles (Fig. 1Ba). Expression of dynamin 2 WT had no visible effect on lamellipodia formation or the structure of the actin cytoskeleton compared to those of control cells (Fig. 1Bb). By contrast, in 555Δ3-expressing and K562E-expressing cells, lamellipodia formation, as determined by the method described in Syriani et al [12], was inhibited by approximately 50%, whereas the effect on actin structures differed in each mutant (Fig. 1C). In K562E expressing cells, radially arranged actin bundles became undetectable concomitant with the appearance of F-actin clusters (Fig. 1Bd and D), whereas actin structures remained unchanged in 555Δ3-expressing cells (Fig. 1Bc). A decrease in stress fibers, actin bundles and the appearance of F-actin clusters were also observed in the absence of serum stimulation in dynamin 2 K562E expressing cells (Supplementary Fig. 1A and B). These results indicated a marked effect of the K562E mutation on the actin cytoskeleton.

Based on the strong effect of the K562E mutation on F-actin distribution, we next examined the subcellular localization of the K562E mutant by immunofluorescence microscopy. WT dynamin 2 showed a fine punctate distribution that partially overlapped with F-actin (5.9 ± 1.0%), consistent with a previous report [13] (Fig. 2A upper panels and 2B). K562E mutant-expressing cells showed colocalization of

dynamin 2 with F-actin clusters by 50.2 ± 3.4% (Fig. 2A lower panels and 2B). Since dynamin 2 functions in endocytosis at endocytic pits together with clathrin and the clathrin adaptor AP-2, we next examined the effect of dynamin 2 mutations on the colocalization of these proteins. Approximately 50% of dynamin 2 WT positive puncta were positive for AP-2 or clathrin (Fig. 2C, 2D and Supplementary Fig. 2), whereas colocalization was decreased to 20% in K562E-expressing cells (Fig. 2C, 2D and Supplementary Fig. 2). Unlike F-actin, the distribution of AP-2 was not affected by the dynamin mutation. These results suggested that dynamin 2 K562E has a greater effect on actin dynamics than on the endocytic machinery.

To confirm that the effect of dynamin 2 K562E on actin cytoskeleton is intrinsic, the same mutant was expressed in HeLa cells. The expression of dynamin 2 K562E in HeLa cells also induced defective of actin bundles, and the appearance of F-actin clusters (Supplementary Fig. 3). In addition, the colocalization of F-actin clusters with dynamin 2 K562E similar to the case in U2OS cells was also observed (Supplementary Fig. 4). In addition, the aberrant F-actin clusters were also observed in K562E mutant expressing NG108-15 cells, mouse neuroblastoma x rat glioma cell line (Supplementary Fig. 5). These results supported that the effect of dynamin 2 K562E on actin cytoskeleton represents intrinsic effect of the mutant.

3.2. Expression of the K562E mutant affects actin dynamics

The aberrant F-actin distribution and defective lamellipodia formation in K562E mutant-expressing cells (Fig. 1) suggested a potential effect of the mutation on actin dynamics near the plasma membrane. To characterize the effect of K562E expression on actin dynamics, live imaging of intracellular F-actin was performed using TIRFM. Long linear F-actin filaments showed twitching movements at the cell periphery (Supplementary movie S1) and assembled into radially aligned thick actin bundles at approximately 20 min after serum stimulation in dynamin WT-expressing cells (Fig. 3A, upper panels). Transverse F-actin bundles were also observed (Fig. 3A upper panel at 36 min), consistent with the results of the phalloidin-staining experiment shown in Fig. 1Bb.

In K562E-expressing cells, F-actin filaments were short and visualized as dots at the cell periphery (Fig. 3A, lower panels). At approximately 20 min after serum stimulation, the short actin filaments assembled, and clear F-actin clusters were formed at approximately 30 min in dynamin 2 K562E-expressing cells (Supplementary movie S2, Figure 3A, lower panels, arrowheads). The F-actin clusters were immobile and persisted throughout the observation. Radially aligned F-actin bundles were almost undetectable, whereas the formation of transversely arranged F-actin bundles was similar to that in dynamin 2 WT-expressing cells (Fig. 3A lower panel at 36 min).
Higher magnification images (Fig. 3B) show actin bundles intersecting at right angles in dynamin 2 WT-expressing cells, whereas in dynamin 2 K562E-expressing cells, F-actin clusters consisted of tangled actin filaments that were not connected to the transverse actin bundles (Fig. 3B, right).
These results indicated that the K562E mutation disrupted actin dynamics at the plasma membrane.

4. Discussion

Dynamin 2 is the disease-causing gene for DI-CMTB [2]. Dynamin 2 CMT mutations disturb clathrin-mediated endocytosis of transferrin or EGF receptors [2, 10, 11] and result in dynamic instability of microtubules [5].

In the present study, we explored the effect of two dynamin 2 CMT mutants, 555Δ3 or K562E, on dynamin function and the actin cytoskeleton. Expression of the dynamin 2 K562E mutant in U2OS cells significantly inhibited the formation of radially aligned actin bundles and caused a loss of higher order actin structures, which consist of actin bundles crossing at right angles (Fig. 1). These changes were accompanied by the appearance of F-actin clusters composed of tangled actin filaments (Fig. 1). Live imaging analyses showed shorter and less dynamic actin filaments in K562E mutant-expressing cells than in WT dynamin-expressing cells upon serum stimulation (Fig. 3). The decreased formation of lamellipodia in K562E-expressing cells may have been caused by these changes of actin dynamics (Fig. 1).

Myelination consists of the coating of axons with layers of myelin derived from

Schwann cells in peripheral neurons or oligodendrocytes in central neurons [14]. Recent studies showed that myelination requires actin remodeling in Schwann cells [15] and oligodendrocytes [16]. Dynamins are directly and indirectly implicated in actin dynamics [17]. Actin bundling by dynamin and cortactin, an F-actin binding protein, stabilizes growth cone filopodia [6]. Intracellular F-actin organization involves crosslinking of F-actin by dynamin and cortactin [7]. In addition, dynamin alone directly binds actin filaments, which changes the higher order structure of F-actin [8]. It is conceivable that dynamin CMT mutations affect actin dynamics during the process of myelination. This hypothesis is supported by evidence that dynamin 2 CMT mutations, including K562E, suppress myelination in Schwann cells [11].

The K562E mutation leads to severe inhibition of endocytic activity [2,10,11], as shown by defects in the recruitment of the mutant protein to the plasma membrane [18]. In the present study, the recruitment of the dynamin 2 K562E mutant to endocytic pit was drastically decreased (Fig. 2 and Supplementary Fig. 2), supporting previous findings. Considering that actin remodeling is implicated in clathrin-mediated endocytosis [19], perturbation of actin dynamics by the K562E mutation may contribute to its inhibitory effect on endocytosis.

The 555Δ3 mutation was shown to cause instability of tubulin dynamics but not actin dynamics [5]. In the present study, 555Δ3 mutant-expressing cells showed defective lamellipodia formation with no obvious change of actin distribution. The inhibitory effect on lamellipodia formation could be attributed to tubulin disarray.

U2OS and HeLa cells were used in this study to assess the effect of the dynamin CMT-mutants on actin dynamics. These cells are widely utilized in dynamin-dependent cellular function. In addition, we found that NG108-15 cell, a mouse neuroblastoma x rat glioma hybrid cell line, showed similar aberrant dynamin and actin localization. However, the cell dependent-effect of dynamin CMT mutant in clathrin-mediated endocytosis has been observed [11]. Analyses of other cell types including neurons, Schwann cells are required for investigating causality of illness for CMT mutation in the future study.

In conclusion, we show for the first time that expression of the dynamin 2 CMT mutant K562E leads to aberrant F-actin distribution as well as lamellipodia formation. These results indicate that disturbance of actin dynamics in dynamin 2 CMT mutants should be considered as a potential mechanism involved in the pathogenesis of CMT.

Acknowledgments

This work was supported by a Grant-in-Aid for Scientific Research from the Ministry of Education, Science, Sports and Culture of Japan (Grant No. 26670201 to H.Y.; Grant No. 15K1533007 to K.T.).

References

[1] A. Patzkó , M.E. Shy, Update on Charcot-Marie-Tooth disease, Curr. Neurol. Neurosci. Rep. 11 (2011) 78-88.

[2] S. Züchner, M. Noureddine, M. Kennerson, K. Verhoeven, K. Claeys, P. De Jonghe, J. Merory, S.A. Oliveira, M.C. Speer, J.E. Stenger, G. Walizada, D. Zhu, M.A. Pericak-Vance, G. Nicholson, V. Timmerman, J.M. Vance, Mutations in the pleckstrin homology domain of dynamin 2 cause dominant intermediate Charcot-Marie-Tooth disease, Nat. Genet. 37 (2005) 289-294.

[3] H. Cao, F. Garcia, M.A. McNiven, Differential distribution of dynamin isoforms in mammalian cells, Mol. Biol. Cell 9 (1998) 2595-2609.

[4] S.M. Ferguson, P. De Camilli P, Dynamin, a membrane-remodelling GTPase, Nat Rev Mol Cell Biol 13 (2012), 75-88.

[5] K. Tanabe, K. Takei, Dynamic instability of microtubules requires dynamin 2 and is impaired in a Charcot-Marie-Tooth mutant, J. Cell Biol. 185 (2009) 939-948.

[6] H. Yamada, T. Abe, A. Satoh, N. Okazaki, S. Tago, K. Kobayashi, Y. Yoshida, Y. Oda, M. Watanabe, K. Tomizawa, H. Matsui, K. Takei, Stabilization of actin bundles by a dynamin 1/cortactin ring complex is necessary for growth cone filopodia, J. Neurosci. 33 (2013) 4514-4526.

[7] O.L. Mooren, T.I. Kotova, A.J. Moore, D.A. Schafer, Dynamin2 GTPase and cortactin remodel actin filaments, J. Biol. Chem. 284 (2009) 23995-24005.

[8] C. Gu, S. Yaddanapudi, A. Weins, T. Osborn, J. Reiser, M. Pollak, J. Hartwig, S. Sever, Direct dynamin-actin interactions regulate the actin cytoskeleton, EMBO J. 29 (2010) 3593-3606.

[9] A.M. González-Jamett, V. Haro-Acuña, F. Momboisse, P. Caviedes, J.A. Bevilacqua, A.M. Cárdenas, Dynamin-2 in nervous system disorders, J. Neurochem. 128 (2014) 210-223.

[10] Y.W. Liu, V. Lukiyanchuk, S.L. Schmid, Common membrane trafficking defects of disease-associated dynamin 2 mutations, Traffic 12 (2011) 1620-1633.

[11] P.N. Sidiropoulos, M. Miehe, T. Bock, E. Tinelli, C.I. Oertli, R. Kuner, D. Meijer, B. Wollscheid, A. Niemann, U. Suter, Dynamin 2 mutations in Charcot-Marie-Tooth neuropathy highlight the importance of clathrin-mediated endocytosis in myelination, Brain. 135 (2012) 1395-1411.

[12] E. Syriani, A. Gomez-Cabrero, M. Bosch, A. Moya, E. Abad, A. Gual, X. Gasull, M. Morales, Profilin induces lamellipodia by growth factor-independent mechanism, FASEB J 22 (2008) 1581-1596.

[13] H. Yamada, T. Abe, S.A. Li, Y. Masuoka, M. Isoda, M. Watanabe, Y. Nasu, H. Kumon, A. Asai, K. Takei, Dynasore, a dynamin inhibitor, suppresses lamellipodia formation and cancer cell invasion by destabilizing actin filaments, Biochem. Biophys. Res. Commun. 390 (2009) 1142-1148.

[14] M. Simons, J. Trotter, Wrapping it up: the cell biology of myelination, Curr Opin Neurobiol 17 (2007) 533-540.

[15] L. Montani, T. Buerki-Thurnherr, J.P. de Faria, J.A. Pereira, N.G. Dias, R. Fernandes, A.F. Gonçalves, A. Braun, Y. Benninger, R.T. Böttcher, M. Costell, K.A. Nave, R.J. Franklin, D. Meijer, U. Suter, J.B. Relvas, Profilin 1 is required for peripheral nervous system myelination, Development 141 (2014) 1553-1561.

[16] S. Nawaz, P. Sánchez, S. Schmitt, N. Snaidero, M. Mitkovski, C. Velte, B.R. Brückner, I. Alexopoulos, T. Czopka, S.Y. Jung, J.S. Rhee, A. Janshoff, W. Witke, I.A. Schaap, D.A. Lyons, M. Simons, Actin filament turnover drives leading edge growth during myelin sheath formation in the central nervous system, Dev. Cell 34 (2015) 139-151.

[17] S. Sever, J. Chang, C. Gu, Dynamin rings: not just for fission, Traffic. 14 (2013) 1194-1199.

[18] J.A. Kenniston, M.A. Lemmon, Dynamin GTPase regulation is altered by PH domain mutations found in centronuclear myopathy patients, EMBO J 29 (2010) 3054-3067.

[19] S.M. Ferguson, A. Raimondi, S. Paradise, H. Shen, K. Mesaki, A. Ferguson, O. Destaing, G. Ko, J. Takasaki, O. Cremona, E. O' Toole, P. De Camilli, Coordinated actions of actin and BAR proteins upstream of dynamin at endocytic clathrin-coated pits, Dev Cell 17 (2009) 811-822.

Figure legends

Fig. 1. Expression of the dynamin 2 CMT mutant K562E results in the formation of aberrant stress fibers, actin bundles, and lamellipodia in serum-stimulated U2OS cells.

(A) Domain structure of dynamin 2 and CMT mutations in rat dynamin 2.

(B) Actin filament localization in CMT mutant dynamin-expressing cells. U2OS cells were transfected with WT (b), 555Δ3 (c), or K562E (d) expression constructs cloned into the pIRES-DsRed2 vector. Untransfected cells are shown in (a) as controls. The cells stimulated with 10% FBS/DMEM for 40 min were fixed, permeabilized, and stained with Alexa Fluor 488-phalloidin. Boxed areas in the top panels correspond to enlarged images of the middle panels. Note a significant decrease of actin bundles and stress fibers, and the presence of F-actin clusters (arrowheads) in K562E mutant-expressing cells (right panels). Dynamin-transfected cells were identified by DsRed2 expression (bottom panels). Bars: 20 μm (top and bottom panels) and 4 μm (middle panels).

(C) Ratio of cells with lamellipodia to total counted cells (** $p<0.01$).

(D) The number of F-actin clusters in the indicated cells was counted (** $p<0.01$).

Fig. 2. The dynamin 2 K562E mutant-induced F-actin clusters co-localize with mutant dynamin but not with clathrin-coated pit marker proteins.

(A) Localization of the dynamin 2 K562E mutant and F-actin clusters. The dynamin 2 WT or K562E mutant-expressing serum-stimulated U2OS cells were stained with Alexa Fluor 488-phalloidin or anti-V5-antibodies and subjected to immunofluorescence analysis. Boxed areas in merged images were enlarged (right). Dynamin 2 K562E colocalized with F-actin clusters (arrowheads). Bars: 20 μm and 5 μm in enlarged panels.

(B) Colocalization of the dynamin 2 K562E mutant with F-actin clusters. The ratio of dynamin 2 K562E mutant positive puncta overlapped with F-actin clusters to total dynamin 2 K562E mutant positive dots was quantified using Metamorph image analysis software. (**: $p<0.01$).

(C) Localization of the dynamin 2 K562E mutant and AP-2. The WT or mutant-expressing cells were stimulated with serum as in A, stained for V5 or AP-2, and analyzed by immunofluorescence. AP-2 was visualized with rhodamine-conjugated

secondary antibodies. Boxed areas in merged images were enlarged (right). Bars: 20 μm and 5 μm in enlarged panels.
(D) Colocalization of the dynamin 2 WT or K562E mutant with AP-2. The ratio of dynamin 2 K562E mutant positive puncta overlapped with AP-2 to total K562E mutant positive dots was quantified using Metamorph image analysis software. (**: $p<0.01$).

Fig. 3. Actin dynamics is disturbed in dynamin 2 K562E mutant-expressing cells.
(A) Representative live-cell time-lapse images of U2OS cells expressing dynamin 2 WT (upper panels) or K562E (lower panels) obtained using Total Internal Reflection Fluorescence microscopy (TIRFM). FBS (10%) was added at 0 min to the culture medium. Bar: 10 μm.
(B) Higher order F-actin structures in dynamin 2 WT (left) or K562E (right) expressing cells. Images acquired at 38 min 20 sec were enlarged. Note the newly formed F-actin aggregates showing a globular shape caused by K562E expression. Bar: 5.5 μm.